

MAXWELLIAN FIELD EXPANSION OF HELICAL MAGNET

K. Hatanaka, T. Katayama*, and T. Tominaka**

Research Center for Nuclear Physics, Osaka University, Ibaraki, Osaka 567, Japan

*Research Center for Nuclear Science, University of Tokyo, Tanashi, Tokyo 188, Japan

**The Institute of Physical and Chemical Research (RIKEN), Wako, Saitama 351-01, Japan

Abstract

Three dimensional (3D) magnetic field calculated by the computer code TOSCA was analyzed including the fringing field region. The magnetic field in the median plane was well simulated by a simple function. Off median plane, contributions from the coils should be taken into account.

1 INTRODUCTION

Superconducting helical dipole magnets will be used in RHIC as Siberian snakes and rotators[1]. Extensive investigations are performed on the orbit and spin trackings to examine whether the spin polarization of the proton will be conserved up to the highest energies with the help of Siberian snakes. During the first stage, the numerical tracking was performed using an analytical expression for the magnetic field in the snake. It is now required to use a more realistic description for the magnetic field in the snake. Beam trajectory and spin motion can numerically be calculated, provided that the magnetic field map is given along the beam path. However, it is not practical to store the whole field strengths along the helical magnets. Besides, the map has usually some errors. Calculated or measured magnetic field maps may not always satisfy Maxwell's equations. This causes errors in numerical calculations of the orbit and spin matrices; orbit matrices should be symplectic, and spin matrices be unitary. There are following three methods to improve the situation. (1) An approximately symplectic matrix calculated from a field map is transformed into an exactly symplectic one, (2) Small modifications to the field values are performed so as to bring the field satisfy Maxwell's equations, (3) The field is made more Maxwellian by reading only one or two field components from the map and deriving the other components by using appropriate expansion coefficients.

The method (3) is physically more sound[2] and should produce a more symplectic matrix. This strategy was applied to examine three dimensional (3D) magnetic field calculated by the computer code TOSCA including the fringing field region.

2 MULTIPOLE EXPANSION OF THE MAGNETIC FIELD

2.1 Cartesian Coordinate System

In a current free region in vacuum where the electric field \vec{E} is constant, the magnetic field \vec{B} can be derived from a scalar potential Ψ as

$$\vec{B} = -\nabla\Psi. \quad (1)$$

In a Cartesian coordinate system, the scalar potential is expanded in power series of x and y coordinates:

$$\Psi = \sum_{m=0}^{\infty} \sum_{n=0}^{\infty} A_{m,n}(z) \frac{x^n}{n!} \frac{y^m}{m!}, \quad (2)$$

where z is a coordinate of axis. If the magnetic field has a median plane symmetry, Ψ is an odd function of y ; i.e., $m = \text{odd}$ [3]. The Laplace equation, $\Delta\Psi = 0$, gives the following recurrent relation between coefficients:

$$A_{m,n+2}(z) + A_{m+2,n}(z) + A_{m,n}^{(2)}(z) = 0. \quad (3)$$

Coefficients, $A_{0,n}(z)$ and $A_{1,n}(z)$ are obtained as functions of z , from the expansion of $B_x(x,0,z)$ and $B_y(x,0,z)$ in the median plane in series of x at each z -position. Therefore, all the coefficients are determined from the analysis of measured/calculated magnetic field distributions only in the median plane:

$$A_{0,n} = -\left(\frac{\partial^n B_x}{\partial x^n}\right)_{x=y=0}, \quad (4)$$

$$A_{1,n} = -\left(\frac{\partial^n B_y}{\partial x^n}\right)_{x=y=0}, \quad (5)$$

$$A_{m,n}^{(k)} = \frac{d^k A_{m,n}}{dz^k}. \quad (6)$$

With these coefficients, $B_x(x,y,z)$, $B_y(x,y,z)$ and $B_z(x,y,z)$ are calculated off median plane as below:

$$B_x = -\frac{\partial\Psi}{\partial x} = -\sum_{m=0}^{\infty} \sum_{n=0}^{\infty} A_{m,n+1}(z) \frac{x^n}{n!} \frac{y^m}{m!}, \quad (7)$$

$$B_y = -\frac{\partial\Psi}{\partial y} = -\sum_{m=0}^{\infty} \sum_{n=0}^{\infty} A_{m+1,n}(z) \frac{x^n}{n!} \frac{y^m}{m!}, \quad (8)$$

$$B_z = -\frac{\partial\Psi}{\partial z} = -\sum_{m=0}^{\infty} \sum_{n=0}^{\infty} A'_{m,n}(z) \frac{x^n}{n!} \frac{y^m}{m!}. \quad (9)$$

2.2 Cylindrical Coordinate System

In the central region of a helical dipole magnet or for a helical magnet of infinite length, the magnetic field has a cylindrical symmetry and a solution of the Laplace equation $\Delta\Psi = 0$ is given by[4]

$$\Psi = -B_0 \left\{ \sum_{n=0}^{\infty} \frac{2^{n+1}(n+1)!}{(n+1)^{n+2}} \frac{1}{r_0^n k^{n+1}} I_{n+1}((n+1)kr) \right. \\ \left. \times [\tilde{a}_n \cos((n+1)\tilde{\theta}) + \tilde{b}_n \sin((n+1)\tilde{\theta})] \right\}, \quad (10)$$

where I_n are modified Bessel functions and $\tilde{\theta}$ is defined as

$$\tilde{\theta} = \theta - kz, \quad (11)$$

where $k = 2\pi/\lambda$ and λ is the wave length of the helix. Modified Bessel functions are expanded in the form of the ascending series of r ,

$$I_{n+1}((n+1)kr) = \sum_{j=0}^{\infty} \frac{1}{j!(n+j+1)!} \left(\frac{(n+1)kr}{2}\right)^{2j+n+1}. \quad (12)$$

Now, the magnetic field can be computed as

$$B_r = B_0 \left\{ \sum_{n=0}^{\infty} \frac{2^{n+1}(n+1)!}{(n+1)^{n+1}} \frac{1}{r_0^n k^n} I'_{n+1}((n+1)kr) \right. \\ \left. \times [\tilde{a}_n \cos((n+1)\tilde{\theta}) + \tilde{b}_n \sin((n+1)\tilde{\theta})] \right\}, \quad (13)$$

$$B_\theta = B_0 \left\{ \sum_{n=0}^{\infty} \frac{2^{n+1}(n+1)!}{(n+1)^{n+1}} \frac{1}{r_0^n k^n} \frac{1}{kr} I_{n+1}((n+1)kr) \right. \\ \left. \times [\tilde{b}_n \cos((n+1)\tilde{\theta}) - \tilde{a}_n \sin((n+1)\tilde{\theta})] \right\}, \quad (14)$$

$$B_z = -krB_\theta, \quad (15)$$

$$B_x = B_r \cos(\theta) - B_\theta \sin(\theta), \quad (16)$$

$$B_y = B_r \sin(\theta) + B_\theta \cos(\theta). \quad (17)$$

Multipole coefficients, \tilde{a}_n and \tilde{b}_n are related with a_n and b_n in a two-dimensional approximation (or a straight magnet)[5]:

$$a_n = \tilde{a}_n \cos((n+1)kz) - \tilde{b}_n \sin((n+1)kz), \quad (18)$$

$$b_n = \tilde{a}_n \sin((n+1)kz) + \tilde{b}_n \cos((n+1)kz). \quad (19)$$

If we expand vertical magnetic field components, B_y , in series of r , we obtain

$$B_y/B_0 = \left[1 + \frac{1}{4}(kr)^2 + (\text{higher order of } r^n) \right] \cdot b_0 \\ + \left\{ \left[b_2 - \frac{1}{8}(kr_0)^2 \cdot b_0 \right] \left(\frac{r}{r_0}\right)^2 + (\text{higher order of } r^n) \right\} \cos(2\theta) \\ + \{\text{higher multipoles}\} \quad (20)$$

Helical dipoles have sextupole components originating from the structure[6]. When the magnet length, $\lambda = 240$ cm and the reference radius, $r_0 = 3.5$ cm, then the sextupole contribution from the dipole field becomes

$$\frac{1}{8}(kr_0)^2 \simeq 1 \times 10^{-3}. \quad (21)$$

3 NUMERICAL ANALYSIS

3.1 Fitting Procedure

In order to analyze the magnetic field calculated by Okamura[7], the scalar potential was assumed to be expanded as

$$\Psi = -B_0 \sum_{n=0}^{\infty} \left(\frac{1}{r_0}\right)^n \\ \times \left\{ \left[\sum_{j=0}^{\infty} \frac{r^{n+1}}{n+2j+1} \left(\frac{r}{r_0}\right)^{2j} \cdot a_{n,j}(z) \right] \cos((n+1)\theta) \right. \\ \left. + \left[\sum_{j=0}^{\infty} \frac{r^{n+1}}{n+2j+1} \left(\frac{r}{r_0}\right)^{2j} \cdot b_{n,j}(z) \right] \sin((n+1)\theta) \right\}. \quad (22)$$

Here, $a_{n,j}(z)$ and $b_{n,j}(z)$ are functions of z , and they are $\cos((n+1)kz)$ - or $\sin((n+1)kz)$ - like functions for an infinitely long magnet. The order of magnitude of their derivatives are estimated as

$$a_{n,j}^{(2m)}(z) = \frac{d^{2m}}{dz^{2m}} a_{n,j}(z) = o(((n+1)k)^{2m}) \cdot a_{n,j} \\ \sim o(10^{-3m}(n+1)^{2m}) \cdot a_{n,j}. \quad (23)$$

From the Laplace equation, $\Delta\Psi = 0$, coefficients, $a_{n,j}(z)$ and $b_{n,j}(z)$, satisfy following relations

$$a_{n,j+1} = -\frac{n+2j+3}{4(j+1)(n+j+2)} \cdot \frac{1}{n+2j+1} \cdot a_{n,j}^{(2)}, \quad (24)$$

$$b_{n,j+1} = -\frac{n+2j+3}{4(j+1)(n+j+2)} \cdot \frac{1}{n+2j+1} \cdot b_{n,j}^{(2)}. \quad (25)$$

In the analysis, coefficients, $a_{n,j}(z)$ and $b_{n,j}(z)$, were determined by fitting the radial field B_r and the azimuthal field B_θ in the median plane ($\theta = 0$ or π), respectively. In the fitting procedure, the maximum value of n was taken 6 and odd n values were also included. The j 's were taken to be zero except for $n = 0$ (dipole component). Only the second derivatives of $a_{0,0}$ and $b_{0,0}$ were taken into account and higher order derivatives were neglected. This assumption is reasonable from the previous estimation of the order of magnitudes for coefficients $a_{n,j}$ and $b_{n,j}$ in (23). Following expansion was used in the fitting procedure,

$$B_r = -\frac{\partial\Psi}{\partial r} \\ = B_0 \left\{ \left[a_{00} + a_{01} \left(\frac{r}{r_0}\right)^2 \right] \cos(\theta) + \left[b_{00} + b_{01} \left(\frac{r}{r_0}\right)^2 \right] \sin(\theta) \right. \\ \left. + \sum_{n=1}^6 \left(\frac{r}{r_0}\right)^n \left[a_{n0} \cos((n+1)\theta) + b_{n0} \sin((n+1)\theta) \right] \right\}, \quad (26)$$

$$B_\theta = -\frac{\partial\Psi}{\partial\theta} \\ = B_0 \left\{ \left[b_{00} + \frac{1}{3}b_{01} \left(\frac{r}{r_0}\right)^2 \right] \cos(\theta) - \left[a_{00} + \frac{1}{3}a_{01} \left(\frac{r}{r_0}\right)^2 \right] \sin(\theta) \right\}$$

$$+ \sum_{n=1}^6 \left(\frac{r}{r_0}\right)^n [b_{n0} \cos((n+1)\theta) - a_{n0} \sin((n+1)\theta)]. \quad (27)$$

The longitudinal field B_z was “predicted” with derivatives of coefficients obtained above,

$$B_z = -\frac{\partial \Psi}{\partial z}$$

$$= B_0 \cdot r \left\{ \left[a'_{00} + \frac{1}{3} a'_{01} \left(\frac{r}{r_0}\right)^2 \right] \cos(\theta) + \left[b'_{00} + \frac{1}{3} b'_{01} \left(\frac{r}{r_0}\right)^2 \right] \sin(\theta) \right.$$

$$\left. + \sum_{n=1}^6 \frac{1}{n+1} \left(\frac{r}{r_0}\right)^n [a'_{n0} \cos((n+1)\theta) + b'_{n0} \sin((n+1)\theta)] \right\}. \quad (28)$$

3.2 Results

At each z -position, coefficients $a_{n0}(z)$ and $b_{n0}(z)$ were determined by fitting the 3D-calculated field B_r and B_θ in the median plane ($y = 0$) with equations (26) and (27). The 3D-field was calculated from x , $y = -35$ mm to 35 mm in 5 mm step including the iron core[7]. Consequently, 14 coefficients were determined by fitting the calculated fields at 30 points with the Simplex minimizing procedure. Differences between the 3D calculated and fitted/predicted fields are shown in Fig. 1. In the median plane, the 3D-field B_x and B_y are well approximated including the fringing field region by the function assuming a cylindrical symmetry. The longitudinal field B_z was “predicted” with the equation (28) and it agrees with the 3D-field very well.

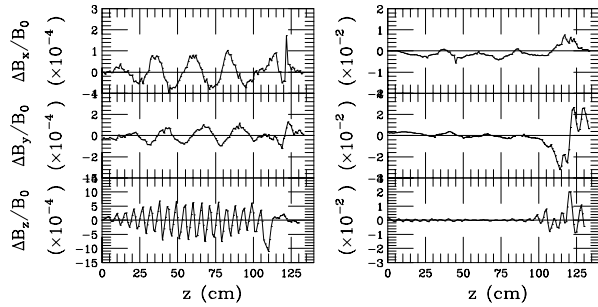


Figure 1: Differences between the 3D-calculated and fitted/predicted fields normalized by B_0 , left: in the median plane $x = 3$ cm and $y = 0$ cm, and right: off median plane $x = 0$ cm and $y = 3$ cm.

Off the median plane, for example along the line $x = 0$ cm and $y = 3$ cm, relatively large differences are observed between 3D-results and our approximation, especially at the magnet edge. The magnetic field generated by a current parallel to the x -axis at $y = y_0$ and $z = z_0$ is given by

$$\vec{B} \propto \left(0, \frac{z - z_0}{[(y - y_0)^2 + (z - z_0)^2]^{\frac{3}{2}}}, \frac{y_0 - y}{[(y - y_0)^2 + (z - z_0)^2]^{\frac{3}{2}}} \right). \quad (29)$$

The fitting errors observed for the B_y field at the magnet edge are well described by the sum of three terms with the functional form (29) corresponding to a magnetic field generated by a line current parallel to the x -axis[8]. Fitting errors for the B_z field at the edge is also described by the functional form derived from three line currents at the same positions, if these currents are reduced by a factor of four[8]. At the edge of a helical magnet, there are currents not only parallel to the x -axis but also those parallel to the z -axis. The latter cause additional B_y field but do not have B_z component. Although the field (29) overestimates the contribution for B_z due to such a simplification, it shows that we have to take account of the effects of the coil at the end of a magnet. Inside the magnet, on the other hand, magnetic field is well described by a simple function of cylindrical symmetry including the fringing field region.

4 SUMMARY

Calculated 3D-field was analyzed to obtain the analytical expressions satisfying Maxwell equations. In the median plane, the field B_x and B_y were well expanded with simple functions of a cylindrical symmetry including the fringing field region. The longitudinal field B_z was also well “predicted” with coefficients determined from fitting B_x and B_y . Off median plane, on the other hand, effects of coils parallel to the x -axis were required to explain the difference between 3D-field and the “predicted” field from the analysis. Present procedure can be also applied to analyze measured magnetic fields for helical magnets.

5 ACKNOWLEDGEMENTS

The authors acknowledge M. Okamura for the results of his 3D calculations, and T. Kawaguchi and A. Luccio for discussions.

6 REFERENCES

- [1] E. Courant et al.: ‘The Use of Helical Dipole Magnets in the RHIC Spin Project’, AGS/RHIC/Spin Note, BNL, No. 40 (1996).
- [2] A. Luccio: ‘Field Map Generated Matrices for Spin Tracking’, AGS/RHIC/Spin Note, BNL, No. 41 (1996).
- [3] K.L. Brown: ‘A First- and Second-Order Matrix Theory for the Design of Beam Transport Systems and Charged Particle Spectrometers’, SLAC Report, No. 75 (1967).
- [4] G.H. Morgan: ‘Computation of the Harmonics in a Helically Wound Multipole Magnet’, AGS/RHIC/Spin Note, BNL, No. 9 (1995).
- [5] W. Fischer: ‘On Measurements of Helical Magnetic Fields Using Devices for Straight Magnets’, AGS/RHIC/Spin Note, BNL, No. 32 (1996).
- [6] T. Katayama: ‘Multipole Field Expansion of Helical Magnet’, AGS/RHIC/Spin Note, BNL, No. 38 (1996).
- [7] M. Okamura: private communication.
- [8] K. Hatanaka: ‘Magnetic Field Analysis of Helical Magnets’, AGS/RHIC/Spin Note, BNL, No. 37 (1996).